NorWeST Stream Temperature Modeling Procedures

Version 3.0; September 15, 2016

http://www.fs.fed.us/rm/boise/AWAE/projects/NorWeST.html

1. Stream temperature metric predicted in NorWeST regional model. An August mean stream temperature was the metric selected to be modeled in the NorWeST temperature model. Use of this metric allowed the largest proportion of data in the NorWeST database to be used, which facilitated calibration of the model to thousands of unique stream sites across the region. Other metrics were considered but the strong correlation among many summer (Table 1) and annual temperature metrics (Table 2) suggest that an August mean conveys much of the information regarding a stream's thermal regime. Moreover, stream temperature monitoring has been historically inconsistent during months other than August, so fitting the model to other periods significantly decreases the number of stream sites used in model calibration. Other factors considered when selecting a temperature metric were the ease with which August mean temperatures could be cross-referenced to similar summaries of climate predictors (e.g., air temperature and stream discharge) and the biological relevance of the August period, which is generally seen as limiting due to high temperatures and low discharge. Finally, the large size of the NorWeST temperature database, combined with the computational intensity of fitting the spatial statistical models, put a premium on limiting the number of temperature metrics that were modeled. Those wishing to derive and model other metrics for specific river basins can do so relatively easily using the raw temperature data provided through the NorWeST website combined with their preferred analytical techniques.

Table 1. Correlations among temperature metrics commonly used to represent summer thermal conditions. Data are from a large temperature database (n = 780 summers of monitoring) compiled for the Boise River basin in central Idaho (Isaak et al. 2010). Definitions of temperature metric acronyms are provided in Dunham et al. (2005).

	Summer mean	MWMT	MWAT	AWAT	AWMT	**August Mean**
Summer mean						
MWMT	0.93					
MWAT	0.98	0.94				
AWAT	1.00	0.93	0.97			
AWMT	0.96	0.98	0.94	0.96		
August Mean	**0.99**	**0.92**	**0.96**	**0.99**	**0.95**	
August MWMT	0.92	0.99	0.92	0.92	0.98	**0.92**

*The strong correlations among metrics means that conversion factors could be developed to translate the August mean temperatures predicted from the NorWeST model as described in Dunham et al. (2005).

Table 2. Correlations among the daily mean and standard deviation of stream temperatures by season from August 1, 2010 – August 31, 2011 at 34 stream sites across the Boise River Basin (D. Isaak, unpublished data). Seasons included summer = June/July/August; fall = Sept/Oct/Nov; winter = Dec/Jan/Feb; and spring = Mar/April/May.

	Annual Mean	Annual SD	Fall mean	Fall SD	Winter Mean	Winter SD	Spring mean	Spring SD	Summer Mean
Annual Mean	---								
Annual SD	0.89	---							
Fall mean	0.98	0.85	---						
Fall SD	0.91	0.94	0.87	---					
Winter Mean	0.45	0.05	0.50	0.02	---				
Winter SD	0.67	0.29	0.70	0.35	0.83	---			
Spring mean	0.97	0.78	0.95	0.76	0.51	0.78	---		
Spring SD	0.80	0.87	0.69	0.77	-0.05	0.29	0.74	---	
Summer Mean	**0.96**	**0.97**	**0.91**	**0.92**	**0.23**	**0.45**	**0.88**	**0.87**	---
Summer SD	0.60	0.77	0.62	0.77	-0.02	0.15	0.48	0.49	0.65

2. Predictors in the NorWeST regional stream temperature model. Ten predictor variables were used in each of the river basin temperature models developed for NorWeST. Two additional predictors (Tailwater and Glacier%) were used in river basins where these factors had strong local influences on August stream temperatures. Two of the 12 predictors (air temperature and stream discharge) were used to represent inter-annual changes in climatic conditions that were common across all sites within a river basin. The remaining 10 predictors represented the spatial characteristics of a river network that affected stream temperatures within an individual year. Interactions among predictor were not included in the final temperature models to ensure the interpretability of parameter estimates and because prescreening suggested minor improvements in the predictive accuracy of the model. The same basic approach to modeling stream temperatures from spatial and temporal predictors was used earlier in Isaak et al. (2010).

A number of spatial predictor variables were derived from the NHDPlus dataset. Early NorWeST processing units were produced using NHDPlusV1 data (USEPA and USGS, 2010), whereas later units used NHDPlusV2 (McKay et al., 2012). For clarity, only information from the NHDPlusV2 dataset (Horizon Systems Corporation, 2012) is cited below. Data content and processing procedures from both datasets are comparable.

1. Air temperature_August (°C). Mean August air temperature for a river basin derived from the dynamically downscaled NCEP RegCM3 reanalysis (Hostetler et al. 2011). Data were downloaded from the USGS Regional Climate Downscaling website (http://regclim.coas.oregonstate.edu/index.html). Stream temperature measurements within a year were cross referenced to the average August air temperature for the same year.

2. Stream discharge_August (m^3/s). Mean August stream discharge for a river basin derived by averaging across USGS flow gages with long-term records and minimal water abstraction or storage reservoirs. Data were downloaded from the NWIS website (http://waterdata.usgs.gov/nwis/rt). Stream temperature measurements within a year were cross referenced to the average August discharge for the same year.

3. Elevation (m). Elevation at stream temperature sites was used to represent the vertical trend towards cooler air temperatures and groundwater. Data were obtained from the 30-m resolution National Elevation Dataset (NED) associated with NHDPlusV2 (Horizon Systems Corporation, 2012; McKay et al. 2012).

4. Latitude (m). The y-coordinate at stream temperature sites from the Albers Equal Area projection was used to represent the poleward trend towards cooler air temperatures. Values were derived in ArcGIS (ESRI 2011) and assigned to each NorWeST point location.

5. Canopy %. The percent tree canopy (Version 1.0) variable from the 2001 version of the National Land Cover Database (MRLC-NLCD 2001; Homer et al. 2007) was used to represent stream shade near a temperature site for early NorWeST processing units. Canopy % values in areas with recent wildfires between 2001 and 2008 were modified based on U.S. Forest Service burn severity data following procedures developed by Miller et al. (2009). Values were averaged over each 1 km NorWeST stream reach. The NLCD data were downloaded from http://www.mrlc.gov/nlcd2001.php. Later NorWeST processing units used the NLCD 2011 USFS, tree canopy cartographic dataset (MRLC-NLCD 2011, Homer et al. 2015).

6. Cumulative drainage area (km^2). The accumulated drainage area value in NHDPlusV2 (NHDPlus table: CumulativeArea.dbf; NHDPlus Field name: TotDASqKM; NorWeST field name: CUMDRAINAG; Horizon Systems Corporation 2012; McKay et al. 2012) at a stream temperature site was used to represent stream size and amount of insolation. It was assumed that larger watersheds would have larger streams that had been insolated over greater distances and would be less shaded by adjacent riparian vegetation due to their greater width.

7. Stream slope %. The stream channel gradient value for an NHDPlusV2 stream reach (NHDPlus table: elevslope.dbf; NHDPlus field name: SLOPE; NorWest field name: SLOPE) in NHDPlusV2; Horizon Systems Corporation 2012; McKay et al. 2012). It was assumed that slope affects flow velocity and equilibration time to local heating conditions. Steeper slopes, therefore, should negatively affect stream temperatures because conditions further upstream at higher elevations have greater influence on local temperatures.

8. Mean annual precipitation (mm). The mean annual precipitation averaged over the area of each NHDPlusV2 catchment (NHDPlus table: IncrPrecipMA.txt; NHDPlus field name: PrecipV; NorWeST field name: PRECIP; Horizon Systems Corporation 2012; McKay et al. 2012) upstream from a stream temperature site. Areas with high annual precipitation may produce higher water yields that have a cooling effect on streams.

9. Base flow index (BFI). The value of the base flow index (NorWeST field name: BFI; Wolock 2003) at a stream temperature site. Streams with larger baseflows and groundwater contributions are thought to be colder than other streams and potentially less sensitive to climate warming. Data were downloaded from http://ks.water.usgs.gov/pubs/abstracts/of.03-263.htm.

10. Glacier %. The percentage of the upstream catchment area classified as glacier (NorWeST field name: GLACIER; Fountain et al. 2006) at each temperature site. Summaries were computed using a standard flow accumulation routine in a GIS. This predictor represents the local cooling effect that glaciers may have on downstream temperatures. Data were downloaded from http://glaciers.research.pdx.edu/Downloads.

11. Lake %. The value of accumulated open water from the NLCD (MRLC-NLCD 2011) in NHDPlusV2 (NHDPlus table: CumTotNLCD2011.txt; NHDPlus field name: NLCD11PC; NorWeST field name: NLCD11PC; Horizon Systems Corporation 2012; McKay et al. 2012), representing the percentage of the catchment area classified as open water at a temperature site. This predictor represents the warming effect that natural lakes and many reservoirs have on downstream temperatures.

12. Tailwater. A categorical predictor variable coded as 0/1 (NorWeST field name: TAILWATER) to indicate whether a stream temperature site occurred in a reach downstream of a deep reservoir that is anomalously cold due to releases of hypolimnetic waters. Code classification was based on observed temperature records and consultation with biologists familiar with the tailwater.

3. Spatial statistical stream network model used for NorWeST regional model. Stream temperature observations in the NorWeST database came from multiple sources and were often spatially clustered and distributed non-randomly. To address potential issues this could create with autocorrelation and parameter estimate bias, spatial statistical models for stream networks were used with NorWeST data (Ver Hoef et al. 2006; Ver Hoef and Peterson 2010; Peterson et al. 2013). These models account for the unique forms of spatial dependence that occur on stream networks (e.g., longitudinal connectivity, flow-volume, and flow-direction; Peterson and Ver Hoef 2010) and have provided accurate temperature predictions when used with similar stream temperature databases previously (Isaak et al. 2010; Isaak et al. 2014).

The form of the model relating the temperature response metric to predictors is similar to standard linear regression models (e.g., $\mathbf{y} = \mathbf{X\beta} + \mathbf{\varepsilon}$). In both cases, the deterministic mean, $\mathbf{X\beta}$, is modeled using predictor variables known to influence the response, $\mathbf{y}$; in this case stream
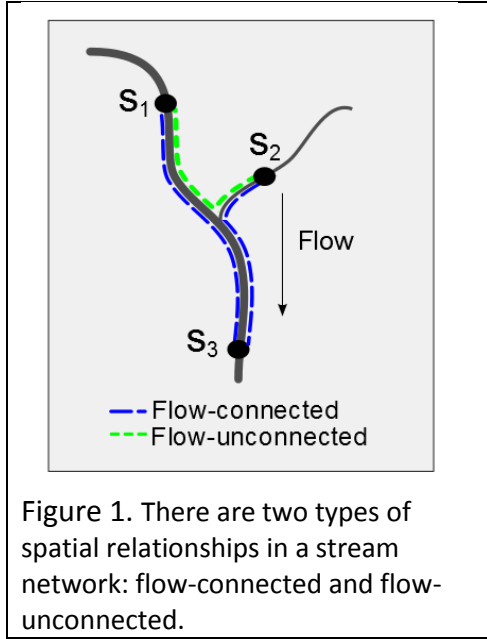

Figure 1. There are two types of spatial relationships in a stream network: flow-connected and flow-unconnected.

temperature. However, the assumption of independence is relaxed in a spatial statistical model to allow spatial autocorrelation in the residual errors, ε. Local deviations from the mean are modeled using the spatial autocorrelation, or spatial covariance, between neighboring sites and a mixture of covariance structures may be used to represent multiple spatial relationships (Peterson and Ver Hoef 2010). For example, there are two types of spatial relationships in a stream network: flow-connected and flow-unconnected. For two locations to be flow-connected, water must flow from an upstream location to a downstream location (S_3 and S_1, S_2 and S_1; Figure 1). Flow-unconnected locations share a common confluence somewhere downstream, but do not share flow (S_2 and S_3; Figure 1). Two covariance models for stream networks have been developed to represent flow-connected and flow-unconnected relationships: the "tail-up" model and the "tail-down" model (Ver Hoef and Peterson 2010). Tail-up covariances are based on hydrologic (e.g., in-stream distance), but restrict spatial correlation to flow-connected sites. In addition, spatial weights are incorporated to account for the disproportionate effects that converging tributaries of differing size or influence may have on downstream areas. Tail-down models allow spatial correlation between both flow-connected and flow-unconnected sites, but a spatial-weighting scheme is not included in this model. When the tail-up, tail-down, and Euclidean covariance models are combined with predictor variables, it provides a robust and flexible modeling framework for streams (Peterson and Ver Hoef 2010). For a detailed description of spatial statistical models for stream networks and the use of a covariance mixture, please see Ver Hoef and Peterson (2010) and Peterson and Ver Hoef (2010).

Three covariance models were used to form a covariance mixture: the exponential tail-up, exponential Euclidean, and the exponential tail-down model. The exponential tail-up autocovariance between flow-connected locations on the stream network is:

$$C_{TU}(s_i, s_j \mid \mathbf{\theta}) = \begin{cases} 0 & \text{if } s_i \text{ and } s_j \text{ are flow-unconnected} \\ \prod_{k \in B_{s_i, s_j}} \sqrt{w_k}\, C_1(h \mid \mathbf{\theta}) & \text{if } s_i \text{ and } s_j \text{ are flow-connected} \end{cases} \quad (1)$$

where

$$C_1(h \mid \mathbf{\theta}) = \sigma_{TU}^2 \exp\left(\frac{-h}{\alpha}\right).$$

5

Here, $\prod_{k \in B_{s_i, s_j}} \sqrt{w_k}$ represents the spatial weights, h is the total hydrologic distance between sites s_i and s_j, and θ is the covariance parameter vector containing $\sigma_{TU}^2 > 0$ (the tail-up partial sill) and $\alpha > 0$ (the range parameter). Also note that $C_I(h| \boldsymbol{\theta})$ is an *unweighted* exponential autocovariance function. When used in the tail-up model, it is not guaranteed to produce a positive definite covariance matrix (a critical requirement of spatial statistical modeling) until it has been weighted appropriately using the spatial weights matrix (Ver Hoef et al. 2006).

The exponential Euclidean autocovariance function is constructed as:

$$C_{TD}\big(s_i, s_j|\theta\big) = \sigma_{TU}^2 \exp(-d/\alpha) \; . \tag{2}$$

Note that (2) is also the tail-down exponential autocovariance function if Euclidean distance, d, is replaced by h. However, this is the only known case where hydrologic distance can be used in a traditional covariance function developed for Euclidean distance and still produce a positive definite covariance matrix (Ver Hoef et al. 2006).

The data needed to fit the spatial models included the stream temperature observations, the 10 predictor variables described in Section 2, x,y coordinates for each location, the hydrologic distance between all sites (both predicted and observed), and spatial weights between all sites. The spatial information used to calculate the hydrologic distances and spatial weights matrices were generated using the STARS ArcGIS toolkit (Peterson and Ver Hoef 2014). The spatial weights were based on watershed contributing area, which was used as a surrogate for stream size. Hydrologic distance and spatial weights matrices were generated using the SSN package (Ver Hoef et al. 2014) in R statistical software prior to fitting the temperature models using the aforementioned package.

4. NorWeST stream temperature scenarios. After the spatial statistical models were fit to the temperature database within a river basin, the model was used to make predictions representing climate scenarios at 1 kilometer intervals throughout the NHDPlus 1:100,000-scale river network. Climate scenarios for historical conditions were created by setting mean August air temperature and stream discharge values to match those observed for a historical period, whether it was an individual year or a composite of multiple years (e.g., 1993-2011). Scenarios $1 - 21$ in Table 3 represent those historic conditions. Future scenarios were developed by adding stream temperature deltas to historical Scenario 1, which represented the composite of years from 1993-2011. Stream temperature deltas consisted of three types: 1) simple integer values (e.g., +1.0˚C, +2.0˚C, +3.0˚C; scenarios 23 - 28); 2) values obtained by multiplying global climate model projections of changes in August air temperatures and discharge by the associated parameters in the stream temperature model (future scenarios 29 and 31), and 3) values based on global climate model projections, which were also adjusted for differential stream sensitivity (future scenarios 30 and 32).

The global climate model projections of August air temperature changes were based on an ensemble mean of the 10 IPCC climate models with the lowest bias in simulating observed climate across the Northwest U.S. (Hamlet et al. 2013). The global climate model simulations were downscaled using a spatially explicit delta method (Hamlet et al. 2010, 2013, in review) to

represent the A1B greenhouse gas emissions trajectory (IPCC 2007) for the 2040s (2030-2059) and 2080s (2070-2099). The same global climate model projections were used with the Variable Infiltration Capacity (VIC) model to generate hydrographs, from which August mean flows were extracted at the USGS gage locations used in stream temperature model development (predictor #2 above). Those data were downloaded when available from the Hydrologic Climate Change website (http://warm.atmos.washington.edu/2860/) developed by the Climate Impacts Group or were derived using identical techniques at other gage locations (Wenger et al. 2010).

Differential sensitivity of streams to climate forcing (i.e., some streams warming more than others) was incorporated by scaling future stream temperature increases relative to the average historical stream temperatures represented by Scenario 1. Basin-specific sensitivity parameters were developed by regressing the observed stream temperatures for each year (1993, 1994, …, 2011) against Scenario 1 predictions at the same site. The slopes of those relationships were then regressed against the network average stream temperature value predicted for the same observation year (Scenarios 3 – 21). The slope of that relationship described the sensitivity of the temperature gradient across a river network relative to inter-annual variation in stream temperatures. That relationship consistently indicated that cold streams were less sensitive than warmer streams as described elsewhere (Luce et al. 2014; Isaak et al. 2016). The stream temperature deltas based on global climate model predictions were used with the sensitivity relationship for a river basin to adjust future temperature gradients while maintaining the same overall stream temperature delta. Incorporating differential stream sensitivity created future scenarios in which the coldest streams often warmed 40% - 60% less than the warmest streams, although differences existing among individual processing units. Figure 2 contrasts the difference between a future scenario that incorporates differential sensitivity and one that does not.
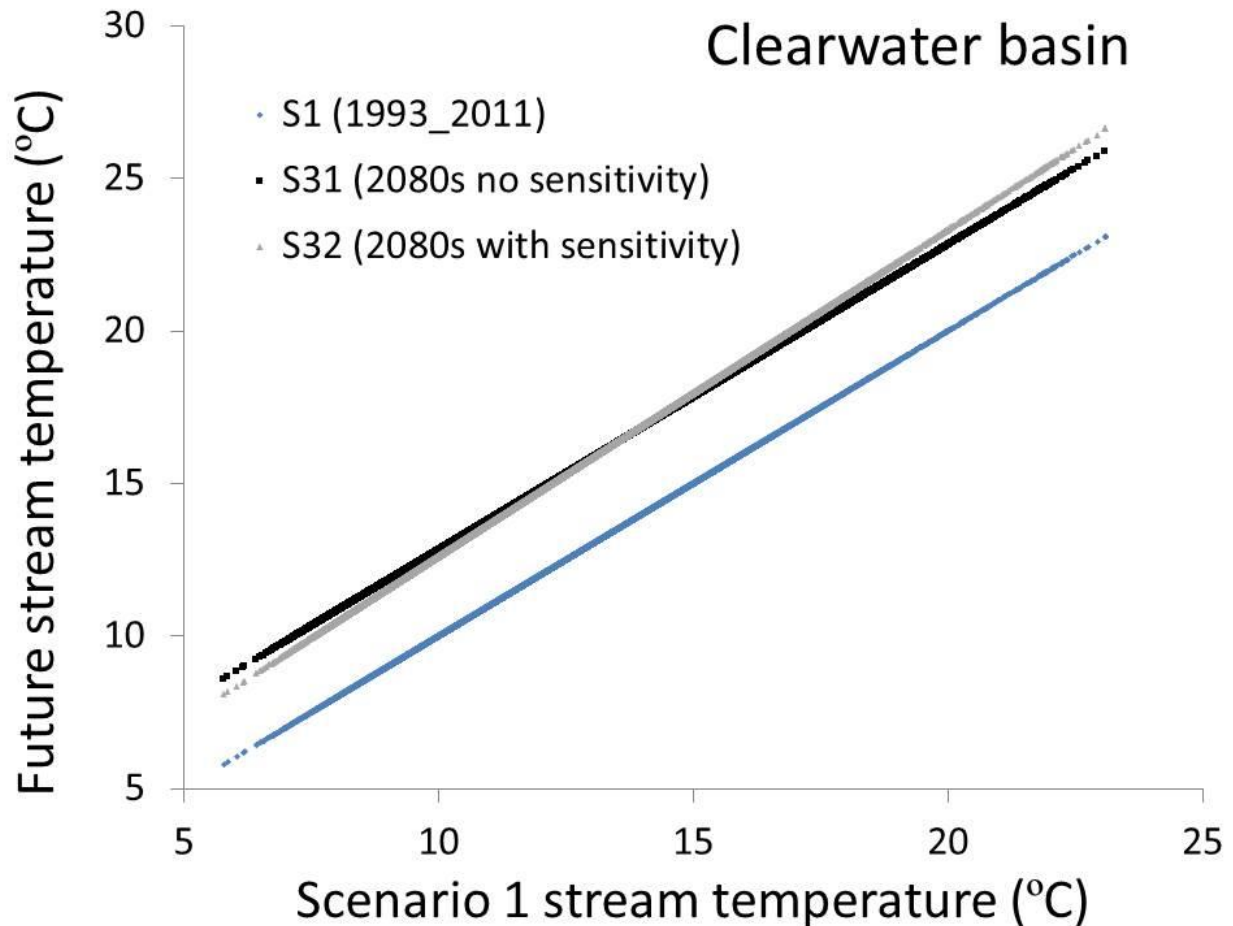
Figure 2. Comparison of NorWeST stream temperature scenarios in the Clearwater River basin. Scenario 1 (1993-2011 composite) provides the historical baseline and scenarios 31 (no differential sensitivity) and 32 (with sensitivity) show the projected changes by 2080 for the A1B warming trajectory.

Table 3. Description of NorWeST historic and future stream temperature climate scenarios.

Scenario	Description
S1_93_11	Historical composite scenario representing 19 year average August mean stream temperatures for 1993-2011
S2_02_11	Historical composite scenario representing 10 year average August mean stream temperatures for 2002-2011
S3_1993	Historical scenario representing August mean stream temperatures for 1993
S4_1994	Historical scenario representing August mean stream temperatures for 1994
S5_1995	Historical scenario representing August mean stream temperatures for 1995
S6_1996	Historical scenario representing August mean stream temperatures for 1996
S7_1997	Historical scenario representing August mean stream temperatures for 1997

S8_1998	Historical scenario representing August mean stream temperatures for 1998
S9_1999	Historical scenario representing August mean stream temperatures for 1999
S10_2000	Historical scenario representing August mean stream temperatures for 2000
S11_2001	Historical scenario representing August mean stream temperatures for 2001
S12_2002	Historical scenario representing August mean stream temperatures for 2002
S13_2003	Historical scenario representing August mean stream temperatures for 2003
S14_2004	Historical scenario representing August mean stream temperatures for 2004
S15_2005	Historical scenario representing August mean stream temperatures for 2005
S16_2006	Historical scenario representing August mean stream temperatures for 2006
S17_2007	Historical scenario representing August mean stream temperatures for 2007
S18_2008	Historical scenario representing August mean stream temperatures for 2008
S19_2009	Historical scenario representing August mean stream temperatures for 2009
S20_2010	Historical scenario representing August mean stream temperatures for 2010
S21_2011	Historical scenario representing August mean stream temperatures for 2011
S22_PredSE	Standard errors of stream temperature predictions
S23_100C	Future scenario adds 1.00°C to S1_93-11
S24_100CD	Future scenario adds 1.00°C to S1_93-11 but also accounts for differential warming of streams by using historical temperatures to scale temperature increases so that cold streams warm less than warm streams.
S25_200C	Future scenario adds 2.00°C to S1_93-11
S26_200CD	Future scenario adds 2.00°C to S1_93-11 but also accounts for differential warming of streams by using historical temperatures to scale temperature increases so that cold streams warm less than warm streams.
S27_300C	Future scenario adds 3.00°C to S1_93-11
S28_300CD	Future scenario adds 3.00°C to S1_93-11 but also accounts for differential warming of streams by using historical temperatures to scale temperature increases so that cold streams warm less than warm streams.

S29_2040	Future August mean stream temperature scenario based on global climate model ensemble average projected changes in August air temperature and stream discharge for the A1B warming trajectory in the 2040s (2030-2059). Future stream deltas are identical at all sites within a NorWeST unit.
S30_2040D	Future August mean stream temperature scenario based on global climate model ensemble average projected changes in August air temperature and stream discharge for the A1B warming trajectory in the 2040s (2030-2059). Future stream deltas within a NorWeST unit account for differential sensitivity among streams so that cold streams warm less than warm streams.
S31_2080	Future August mean stream temperature scenario based on global climate model ensemble average projected changes in August air temperature and stream discharge for the A1B warming trajectory in the 2080s (2070-2099). Future stream deltas are identical at all sites within a NorWeST unit.
S32_2080D	Future August mean stream temperature scenario based on global climate model ensemble average projected changes in August air temperature and stream discharge for the A1B warming trajectory in the 2080s (2070-2099). Future stream deltas within a NorWeST unit account for differential sensitivity among streams so that cold streams warm less than warm streams.
S33_2012	Historical scenario representing August mean stream temperatures for 2012
S34_2013	Historical scenario representing August mean stream temperatures for 2013
S35_2014	Historical scenario representing August mean stream temperatures for 2014
S36_2015	Historical scenario representing August mean stream temperatures for 2015
S37_9311_M	Historical composite scenario representing 19 year average Maximum Weekly Maximum Temperature (MWMT or 7DADM) for 1993-2011
S38_2040_M	Future Maximum Weekly Maximum Temperature (MWMT or 7DADM) stream scenario based on global climate model ensemble average projected changes for the A1B warming trajectory in the 2040s (2030-2059). Future stream deltas are identical at all sites within a NorWeST unit.
S39_2040D_M	Future Maximum Weekly Maximum Temperature (MWMT or 7DADM) stream scenario based on global climate model ensemble average projected changes for the A1B warming trajectory in the 2040s (2030-2059). Future stream deltas within a NorWeST unit account for differential sensitivity among streams so that cold streams warm less than warm streams.

S40_2080_M	Future Maximum Weekly Maximum Temperature (MWMT or 7DADM) stream scenario based on global climate model ensemble average projected changes for the A1B warming trajectory in the 2080s (2070-2099). Future stream deltas are identical at all sites within a NorWeST unit.
S41_2080D_M	Future Maximum Weekly Maximum Temperature (MWMT or 7DADM) stream scenario based on global climate model ensemble average projected changes for the A1B warming trajectory in the 2080s (2070-2099). Future stream deltas within a NorWeST unit account for differential sensitivity among streams so that cold streams warm less than warm streams.

Literature cited:

Dunham, J.B., G. Chandler, B.E. Rieman, and D. Martin. 2005. Measuring stream temperature with digital dataloggers: a user's guide. General Technical Report RMRSGTR-150WWW. U.S. Forest Service, Rocky Mountain Research Station, Fort Collins, Colorado, USA.

ESRI 2011. ArcGIS Desktop: Release 10. Redlands, CA: Environmental Systems Research Institute.

Fountain, A.G., M. Hoffman, K. Jackson, H. Basagic, T. Nylen, and D. Percy, 2006. Digital outlines and topography of the glaciers of the American West. USGS Report 1340.

Hamlet, A.F., M.M. Elsner, G.S. Mauger, S-Y. Lee, I. Tohver, and R.A. Norheim. 2013. An overview of the Columbia Basin Climate Change Scenarios Project: Approach, methods, and summary of key results. Atmosphere-Ocean 51:392-415.

Hamlet, A. F., P. Carrasco, J. Deems, M. M. Elsner, T. Kamstra, C. Lee, S-Y. Lee, G. Mauger, E.P. Salathe, I. Tohver, and L.W. Binder. 2010. Final project report for the Columbia Basin Climate change scenarios project. Retrieved from http://warm.atmos.washington.edu/2860/report/

Hamlet, A.F., E.P. Salathé, and S.J. Burges. In review. A review of three statistical downscaling techniques with application to water resources planning studies in the Pacific Northwest. Journal of the American Water Resources Association

Homer, C., Dewitz, J., Fry, J., Coan, M., Hossain, N., Larson, C., Herold, N., McKerrow, A., VanDriel, J.N., and Wickham, J. 2007. Completion of the 2001 National Land Cover Database for the Conterminous United States. Photogrammetric Engineering and Remote Sensing, 73:337-341.

Homer, C.G., J.A. Dewitz, L. Yang, S. Jin, P. Danielson, G. Xian, J. Coulston, N.D Herold, J.D. Wickham, and K. Megown. 2015, Completion of the 2011 National Land Cover Database for the conterminous United States-Representing a decade of land cover change information. Photogrammetric Engineering and Remote Sensing, v. 81, no. 5, p. 345-354

Horizon Systems Corporation, 2012. NHDPlus Version 2 website. http://www.horizon-systems.com/NHDPlus/index.php, accessed September, 2016.

Hostetler, S.W., J.R. Alder, and A.M. Allan. 2011. Dynamically downscaled climate simulations over North America: Methods, evaluation and supporting documentation for users: U.S. Geological Survey Open-File Report 2011-1238, 64 p. website: http://regclim.coas.oregonstate.edu/index.html

IPCC (Intergovernmental Panel on Climate Change). 2007. Climate change 2007: Working group 2: Impacts, adaptation and vulnerability.

Isaak, D.J., C. Luce, B.E. Rieman, D. Nagel, E. Peterson, D. Horan, S. Parkes, and G. Chandler. 2010. Effects of climate change and recent wildfires on stream temperature and thermal habitats for two salmonids in a mountain river network. Ecological Applications 20:1350-1371.

Isaak, D.J., E. Peterson, J. V. Hoef, S. Wenger, J. Falke, C. Torgersen, C. Sowder, A. Steel, M.J. Fortin, C. Jordan, A. Reusch, N. Som, P. Monestiez. 2014. Applications of spatial statistical stream network models to stream data. Wiley Interdisciplinary Reviews - Water 1:277-294.

Isaak, D., M. Young, C. Luce, S. Hostetler, S. Wenger, E. Peterson, J. Ver Hoef, M. Groce, D. Horan, and D. Nagel. 2016. Slow climate velocities of mountain streams portend their role as refugia for cold-water biodiversity. Proceedings of the National Academy of Sciences 113:4374-4379.

Luce, C.H., B. Staab, M. Kramer, S. Wenger, D. Isaak, and C. McConnell. 2014. Sensitivity of summer stream temperature to climate variability in the Pacific Northwest. Water Resources Research 50:3428-3443.

McKay L., Bondelid T., Dewald T. Johnston, J., Moore, R., and Rea, A. 2012. NHDPlus Version 2: User Guide. U.S. Environmental Protection Agency. http://www.horizon-systems.com/NHDPlus/NHDPlusV2_documentation.php, accessed September, 2016.

Miller, J.D., E.E. Knapp, C.H. Key, C.N. Skinner, C.J. Isbell, R.M. Creasy, J.W. Sherlock, 2009. Calibration and validation of the relative differenced Normalized Burn Ratio (RdNBR) to three measures of fire severity in the Sierra Nevada and Klamath Mountains, California, USA. Remote Sensing of the Environment 113:645-656.

MRLC-NLCD, 2001. National Land Cover Data Set available at: http://www.mrlc.gov/nlcd2001.php, accessed September, 2016.

MRLC-NLCD, 2011. National Land Cover Data Set available at: http://www.mrlc.gov/nlcd11_data.php, accessed September, 2016.

Peterson, E.E., and J. M. Ver Hoef. 2014. STARS: An ArcGIS toolset used to calculate the spatial information needed to fit spatial statistical models to stream network data. Journal of Statistical Software 56(2).

Peterson, E.E., J.M. Ver Hoef, D.J. Isaak, J.A. Falke, M.-J. Fortin, C.E. Jordan, K. McNyset, P. Monestiez, A.S. Ruesch, A. Sengupta, N. Som, A. Steel, D.M. Theobald, C.E. Torgersen & S.J. Wenger. 2013. Modeling dendritic ecological networks in space: An integrated network perspective. Ecology Letters 16:707-719.

Peterson, E.E. and J. M. Ver Hoef. 2010. A mixed-model moving-average approach to geostatistical modeling in stream networks. Ecology 91:644-651.

USEPA and USGS. 2010. NHDPlus Version 1 (NHDPlusV1) User Guide, available online at http://www.horizon-systems.com/NHDPlus/NHDPlusV1_documentation.php

Ver Hoef, J.M., E.E. Peterson, D. Clifford, and R. Shah. 2014. SSN: An R package for spatial statistical modeling on stream networks. Journal of Statistical Software 56(3).

Ver Hoef, J.M., and E.E. Peterson. 2010. A moving average approach for spatial statistical models of stream networks. Journal of the American Statistical Association 105:6-18.

Ver Hoef, J.M., E.E. Peterson, and D. Theobald. 2006. Spatial statistical models that use flow and stream distance. Environmental and Ecological Statistics 13:449-464.

Wenger, S.J., C.H. Luce, A.F. Hamlet, D.J. Isaak, and H.M. Neville. 2010. Macroscale hydrologic modeling of ecologically relevant flow metrics. Water Resources Research 46, W09513, doi:10.1029/2009WR008839.

Wolock, D.M. 2003. Base-Flow Index Grid for the Conterminous United States. U.S. Geological Survey open-file report 03-263, USGS, Lawrence, KS.